Project 1, Atmospheric Ray Tracing

Davis McKenzie
Ionospheric Radio

February 17, 2026

The following report prepared for ELEC 6970 - Special Topics: Ionospheric Radio is Structured as follows:

1. Project Motivations
2. Two-Dimensional Ray Tracing Implementation and Results
3. Three-Dimensional Ray Tracing Implementation and Results
4. Anisotropy Analysis Using PHaRLAP
5. Further Uses of PHaRLAP and Ray Tracing

1 Project Motivations

The ionosphere plays a large role in long-distance radio propagation, especially in the high-frequency (HF) range. Using the PHaRLAP toolbox available from the Defence Science and Technology Group of the Australian Department of Defence [1], the behavior of individual propagating rays may be studied. Apart from studying HF propagation, this tool can also be used to learn about how real-world systems, such as ionosondes, make measurements. By extracting useful information such as the maximum height reached by rays and their path data, characteristics of the ionosphere may be deduced in a manner similar to how functional instruments make these determinations. For this project, oblique ionograms are generated by analyzing rays traced from sites in Chesapeake, Virginia, USA and Corpus Christi, Texas, USA.

2 Two Dimensional Ray Tracing Implementation and Results

The `raytrace_2d()` function is available in PHaRLAP to trace rays in a plane located between two points on Earth's surface. An example of the rays traced by this function is shown below in Figure 1. `raytrace_2d()` was used to generate rays for further analysis in this section.

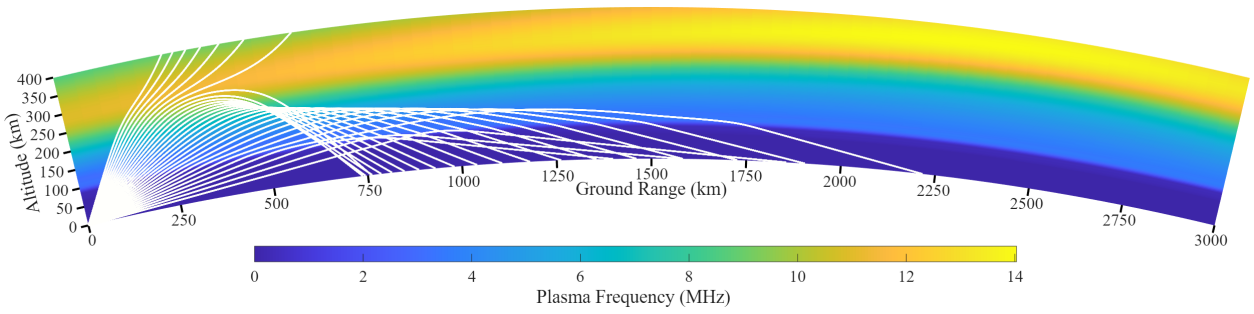

Figure 1: An Example of Rays Traced by the 2D Ray-Tracing function in PHaRLAP.

2.1 Generation of Rays and Ray Data

To generate all necessary inputs for the ray tracing function, a function to calculate the bearing and distance between two coordinate points and Earth was created, `Bearing_Calculator`. Arguments to this function are two points given in degrees, minutes, seconds format using the WGS84 standard, outputs from this function are the true north compass heading pointing from the source location to the destination location, the distance separating the coordinate points, and the source latitude and longitude as signed decimal values. The `Ionospheric_Grid_2D` function is used alongside `Bearing_Calculator` with the former's arguments being source site and destination site, both in degrees, minutes, seconds format, as well as a row vector containing the UTC time at which the rays are desired to be traced.

`Ionospheric_Grid_2D` returns an ionospheric plasma frequency grid, collision frequency, ionospheric electron temperature grid, ionospheric start height, the height increment, the range increment, and the irregularities flag. The plasma frequency grids are then converted to electron number density grids using the relation

$$N_e = \frac{f_p^2}{80.6164 \times 10^{-6}} \tag{1}$$

where f_p is the plasma frequency and N_e is the electron number density. The two-dimensional slice of electron number density formed by the grid is shown below in Figure 2. Using these

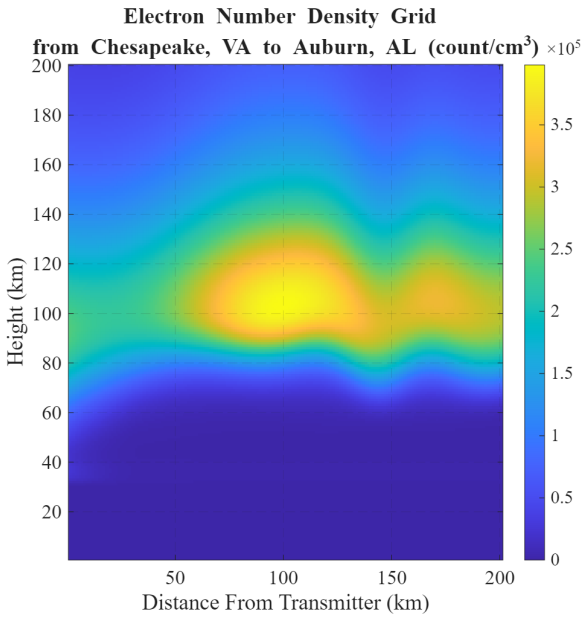

Figure 2: The Ionospheric Grid Generated for 7/1/2004 at 10:00 UTC between Chesapeake, VA and Auburn, AL (Vertical Slice)

outputs, the `raytrace_2d` function can then be called/initialized. Upon first execution, the ionospheric condition values are stored in memory and are therefore not required on subsequent executions. The raytracing model is initialized for some dummy frequency and launch angle before the script uses a loop to complete further runs of the raytracing model for the launch angles of interest across the frequency range of interest.

For the two-dimensional simulation, the source site is set to Chesapeake, Virginia, and the destination (target) is Auburn, Alabama. The time of interest is July 1, 2004 at 10:00 UTC. The initial call to `raytrace_2d` uses a single elevation angle of 20° and a frequency of 5 MHz to initialize the ionospheric model. Subsequent calls sweep elevation angles from 1° to 90° in increments of 0.05° across frequencies from 1 MHz to 20 MHz in increments of 0.1 MHz.

2.2 Ray Filtering and Data Extraction

After each call to `raytrace_2d` at a given frequency, the script must identify which of the many traced rays (across all elevation angles) actually arrive at or near the target location.

To accomplish this, two filtering criteria are applied to the output ray data.

First, the `ray_label` field returned by the raytracing function is checked. A ray label of 1 indicates that the ray has returned to the ground after reflecting from the ionosphere (i.e., it is a valid one-hop ray). Rays that penetrate the ionosphere, are absorbed, or otherwise fail to return to the surface are excluded by this criterion.

Second, the `ground_range` of each valid ray is compared to the known target distance (as calculated by `Bearing_Calculator`). Only rays whose ground range falls within a specified tolerance of the target distance are retained. For the 2D simulation, this tolerance (`max_distance_error`) is set to 5 km. The filtering condition can be expressed as:

$$\texttt{valid} = (\texttt{ray\_label} = 1) \ \wedge \ (|\texttt{ground\_range} - D_{\text{target}}| \leq \Delta D_{\max}) \tag{2}$$

where D_{target} is the great-circle distance to the destination and $\Delta D_{\max}$ is the maximum allowable distance error.

Among all rays that satisfy both conditions at a given frequency, the one whose ground range is closest to the target distance is selected as the representative ray for that frequency. The following quantities are extracted and stored for this best-fit ray: apogee (maximum altitude), ground range, group range, phase path, geometric path length, and the latitude and longitude of the ray's landing point. If no valid ray exists for a particular frequency (indicating that the ionosphere cannot support propagation at that frequency over the given path), all stored values for that frequency are set to NaN.

This process is repeated for every frequency in the sweep, building up arrays indexed by frequency that represent the "best" ray connecting the source and target at each operating frequency. The resulting data is the foundation upon which virtual reflection heights are subsequently calculated.

2.3 Calculation of Virtual Reflection Height

With the path data extracted for each frequency, the next step is to estimate the virtual reflection height of the ionosphere. The virtual height is the height at which a signal would appear to reflect if it were assumed to travel in a straight-line triangular path at the speed of light. This is the same quantity measured by ionosondes and is central to constructing ionograms.

2.3.1 Chord Length Calculation

Because the propagation path follows a curved Earth, the first step is to compute the chord length connecting the source and target beneath the surface. Given the Earth's radius R and the great-circle ground distance D, the chord length is:

$$C = 2R \sin\left(\frac{D}{2R}\right) \tag{3}$$

This chord represents the straight-line base of the assumed isosceles triangular propagation path.

2.3.2 Earth Curvature Correction

The triangular model assumes a flat baseline, but the Earth's surface curves downward between the source and target. The sagitta s quantifies the maximum vertical deviation of the chord from the curved surface at the midpoint of the path:

$$s = R - \sqrt{R^2 - \frac{C^2}{4}} \tag{4}$$

This correction must be subtracted from the calculated triangular height to account for the fact that the apex of the triangle is measured relative to the chord, not the curved surface.

2.3.3 Triangular Height from Path Length

In the simple triangular model, the signal travels from the source up to a virtual reflection point and back down to the target. If the total one-way path length along each leg is $P/2$ (where P is the total path length) and the baseline is C, then by the Pythagorean theorem the virtual height above the chord midpoint is:

$$h_{\text{triangle}} = \sqrt{\frac{P^2 - C^2}{4}} \tag{5}$$

This calculation is performed using three different measures of path length provided by PHaRLAP: group range, phase path, and geometric path length. The group range accounts for the group velocity of the signal through the ionosphere and represents the path length that would be inferred from a time-of-flight measurement. The phase path integrates the refractive index along the geometric path and represents the effective optical path length. The geometric path length is simply the physical distance traveled by the ray regardless of the refractive index.

After computing h_{triangle} for each path type, the Earth curvature correction s is subtracted to yield the corrected virtual height:

$$h_{\text{virtual}} = h_{\text{triangle}} - s \tag{6}$$

2.4 Results and Further Processing

The primary output of the two-dimensional simulation is a plot of ionospheric reflection height versus frequency, forming an oblique ionogram. The plot compares three quantities across the frequency range of 1–8 MHz: the ray trace apogee (the true maximum altitude reached by the ray as reported by PHaRLAP), the calculated virtual height derived from the group path, and the calculated virtual height derived from the geometric path. The ionograms generated for Chesapeake, VA to Auburn, AL and Corpus Christi, TX to Auburn, AL are shown below in Figures 3 and 4, respectively.

The ray trace apogee represents the physical height at which the ray reaches its highest point in the ionosphere. The virtual heights derived from the group and geometric paths, on the other hand, represent the heights that would be inferred from the triangular propagation model. These two calculated heights differ because the group range is affected by the

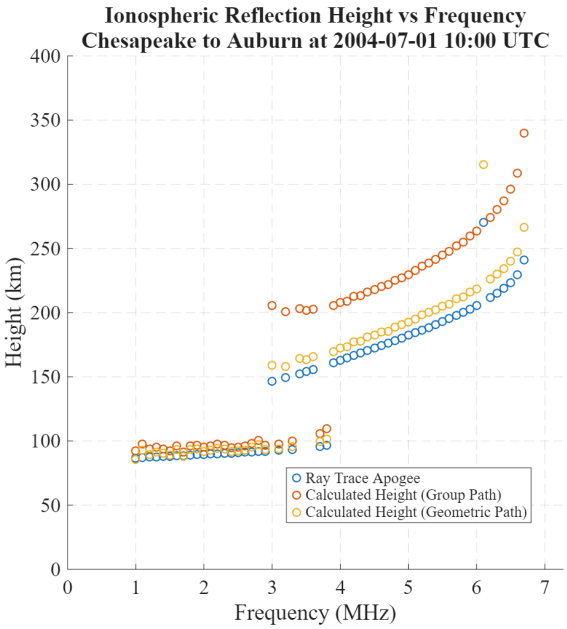

Figure 3: Chesapeake 2D Ionogram

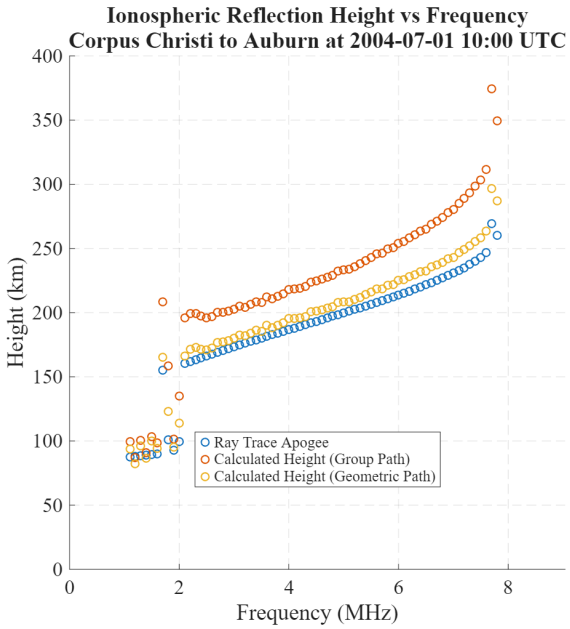

Figure 4: Corpus Christi 2D Ionogram

refractive slowing of the signal in the ionosphere (resulting in a group range that exceeds the geometric path length), while the geometric path length reflects only the true physical distance traveled. As a result, the group-path virtual height is generally higher than the geometric-path virtual height, and both differ from the true apogee.

At lower frequencies, the reflection occurs at lower altitudes (in the E-region or lower F-region), and as frequency increases, the reflection height rises until the maximum usable frequency (MUF) is reached. Beyond the MUF, no valid rays reach the target, and the data contains NaN values, producing a gap in the ionogram. The MUF for the Chesapeake–Auburn path is shown to be roughly 6.75 MHz, while the MUF for the Corpus Christi–Auburn path has a slightly higher MUF at almost 8 MHz.

In addition to the ionogram, a geographic scatter plot is produced showing the landing points of all valid traced rays overlaid on a topographic map. The target location (Broun Hall at Auburn University, approximately 32.6047° N, 85.4867° W) is marked for reference. This visualization provides insight into the ray filtering procedure and can confirm that the selected rays are indeed arriving within the specified tolerance of the target location. The clustering of landing points around the target provides confidence in the validity of the extracted path data.

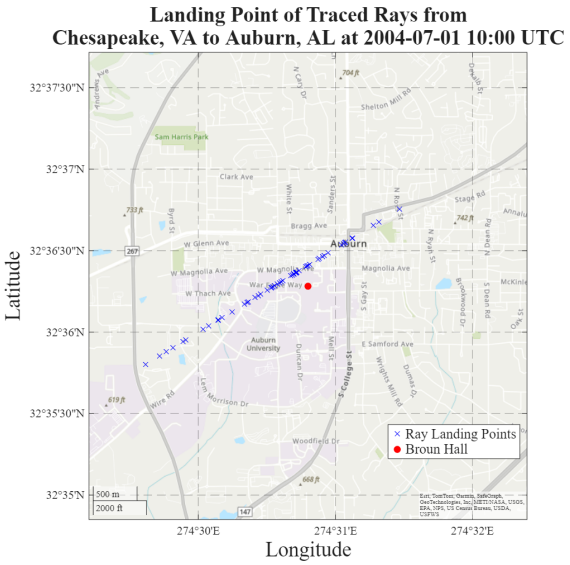

Figure 5: Ray Endpoints from Chesapeake

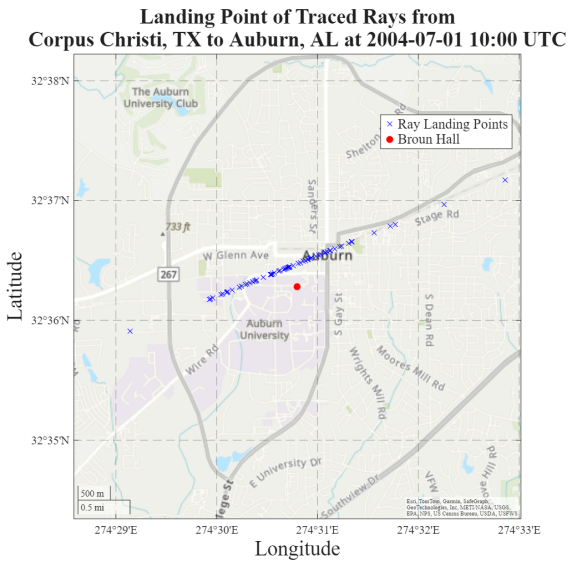

Figure 6: Ray Endpoints from Corpus Christi

3 Three-Dimensional Ray Tracing Implementation and Results

While the two-dimensional ray tracing approach provides useful results, it operates under the assumption of an isotropic ionosphere contained within the vertical plane between the source and destination. In reality, the ionosphere is anisotropic due to the presence of the Earth's geomagnetic field. The `raytrace_3d()` function in PHaRLAP accounts for these effects by tracing rays through a three-dimensional ionospheric model that includes the geomagnetic field, enabling the study of magneto-ionic propagation modes.

3.1 Generation of the 3D Ionospheric Model

The three-dimensional simulation uses the function `Ionospheric_Grid_3D` to generate the ionospheric parameters. Unlike the 2D case, which produces a vertical slice along the propagation path, the 3D grid covers a volume of the ionosphere. In addition to the plasma frequency grid, the 5-minute plasma frequency grid, and the collision frequency, the 3D grid function also returns the three components of the geomagnetic field (B_x, B_y, B_z), the ionospheric grid parameters, and the geomagnetic grid parameters. These additional outputs are required by the 3D ray tracing function to properly model the interaction of the propagating wave with the magnetized plasma.

As in the 2D case, the plasma frequency grids are converted to electron number density grids using the same relation given in Equation (1). The bearing and target distance are again calculated using `Bearing_Calculator`. An initial call to `raytrace_3d` is made with a dummy elevation and frequency, and the full ionospheric and geomagnetic grid data to initialize the ionospheric model in memory for subsequent calls. The origin height is set to 0.0 km (ground level).

3.2 O-Mode and X-Mode Propagation

A key distinction of 3D ray tracing is the ability to separately model the two magneto-ionic propagation modes: the ordinary mode (O-mode) and the extraordinary mode (X-mode). In a magnetized plasma such as the ionosphere, an incident wave splits into these two characteristic modes, each experiencing a different refractive index and therefore following a different path through the medium.

In PHaRLAP, the propagation mode is selected via the `OX_mode` parameter. Setting `OX_mode␣=␣1` traces O-mode rays, while `OX_mode␣=␣-1` traces X-mode rays. For each mode, the script performs a full frequency sweep from 1 MHz to 20 MHz in 0.1 MHz steps, with elevation angles swept from 1° to 90° in 0.05° increments. The ray bearing for all rays is set to the computed azimuth from the source to the target.

The ray filtering and data extraction procedure is identical to the 2D case described in Section 2.2, with the exception that the maximum distance error tolerance is set to 3 km for the 3D simulation. For each frequency and each mode, the ray with a valid return (ray label = 1) whose ground range best matches the target distance is selected, and the same set of quantities (apogee, group range, phase path, geometric path length, landing latitude and longitude) is stored. Separate arrays are maintained for O-mode and X-mode results.

3.3 Virtual Height Calculation for O-Mode and X-Mode

The virtual height calculation proceeds identically to the method described in Section 2.3, applied separately to the O-mode and X-mode path data. The chord length and Earth curvature correction are computed once (since the ground distance is the same for both modes), and then the triangular height formula is applied to the group range, phase path, and geometric path length for each mode independently. This yields six sets of virtual height data: three path-length types for each of two propagation modes.

3.4 Results

The 3D simulation produces several plots for analysis. Figures 7 and 8 show a comparison of the ray trace apogees for O-mode and X-mode for Chesapeake, VA and Corpus Christi, TX to Auburn, AL, respectively. Because the X-mode interacts more strongly with the geomagnetic field, it is reflected at a different (generally lower) electron density than the O-mode, leading to differences in reflection height. At a given frequency, the X-mode ray typically reflects at a lower altitude than the O-mode ray, and the X-mode maximum usable frequency is slightly higher than the O-mode MUF.

Figures 9 and 10 compare the calculated virtual heights derived from the geometric path length for O-mode and X-mode. This pair of curves corresponds to what would be observed on an oblique ionogram produced by a system capable of resolving the two magneto-ionic modes. The separation between the O-mode and X-mode traces can provide information about the geomagnetic field strength and orientation along the propagation path.

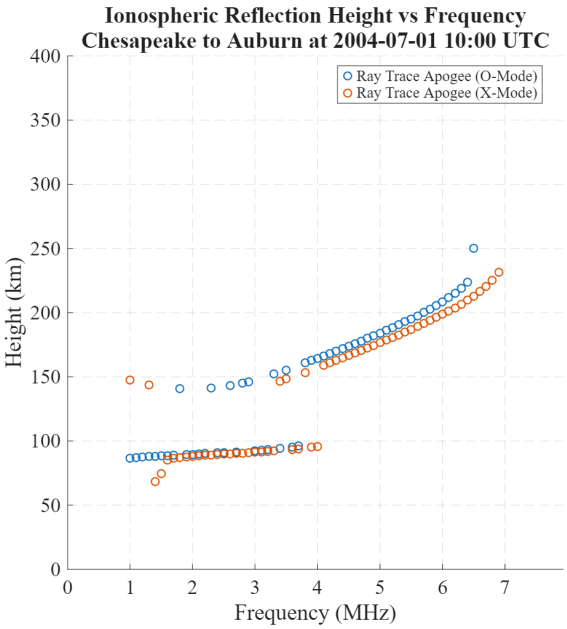

Figure 7: Apogee Ionogram for Chesapeake

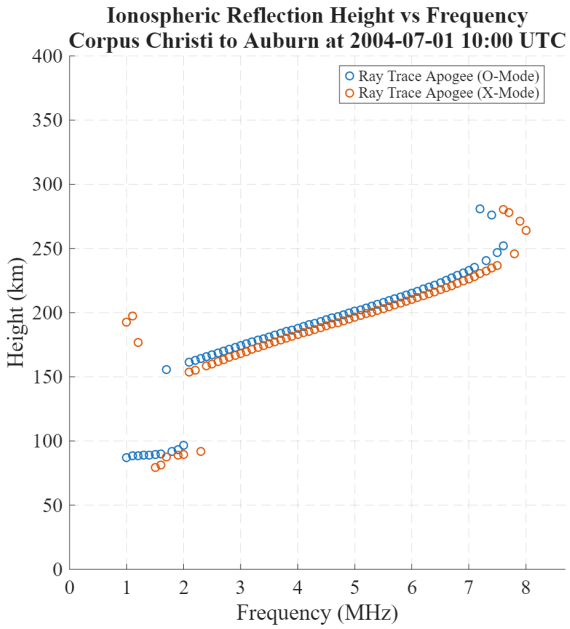

Figure 8: Apogee Ionogram for Corpus Christi

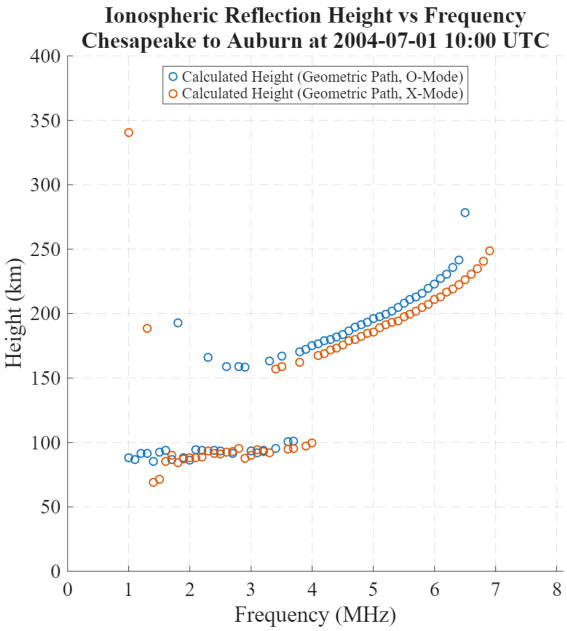

Figure 9: Geometric Path Ionogram for Chesapeake

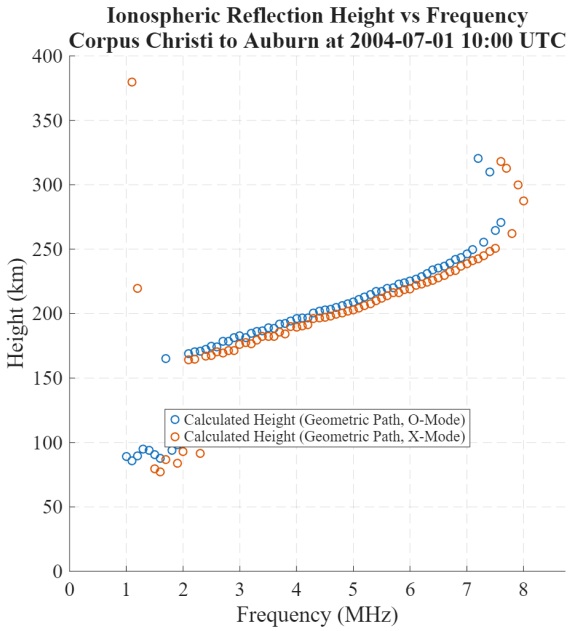

Figure 10: Geometric Path Ionogram for Corpus Christi

Geographic scatter plots are also produced for the 3D case, combining the landing points of both O-mode and X-mode rays. Notably, because the 3D model accounts for lateral deviations caused by the geomagnetic field, the landing points may not lie exactly along the great-circle path between the source and target. Figures 11 and 12 show the landing locations for the rays traced from Chesapeake, VA and Corpus Christi, TX to Auburn, AL, respectively. Through plotting these endpoints, a deficiency in the ray selection process

was discovered. In the 3D ray tracing case, since rays can curve "left" or "right" as they propagate through the ionosphere, the landing site of a ray with the closest distance to the target distance could lie anywhere around a circle with a radius of target distance centered on the transmitter location. In practice, this rarely occurred, with the data not contributing greatly to error. The filtering method, therefore, was maintained for the remaining portions of the assignment.

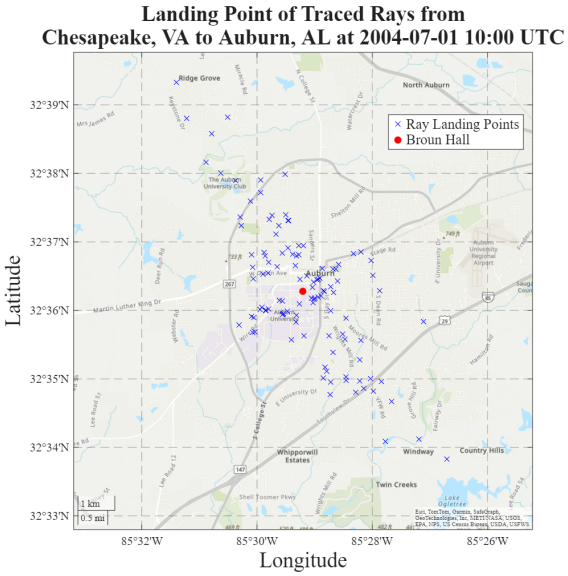

Figure 11: Ray Endpoints from Chesapeake (3D)

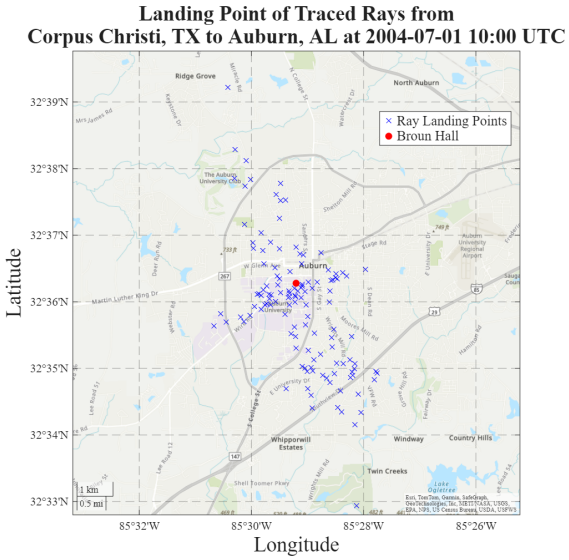

Figure 12: Ray Endpoints from Corpus Christi (3D)

4 Anisotropy Analysis Using PHaRLAP

An important consequence of the geomagnetic field's influence on ionospheric propagation is that the ionosphere is not reciprocal for oblique paths. That is, a signal traveling from site A to site B may experience a different effective ionosphere than a signal traveling from site B to site A. This directional dependence, or anisotropy, arises because the orientation of the wave vector relative to the geomagnetic field changes when the direction of propagation is reversed, leading to different refractive index profiles for the two directions. This section investigates this effect using PHaRLAP's 3D ray tracing capability.

4.1 Methodology

The anisotropy analysis is performed for two propagation paths: Chesapeake, VA ↔ Auburn, AL and Corpus Christi, TX ↔ Auburn, AL. For each path, the full 3D ray tracing procedure described in Section 3 is executed twice: once with the signal propagating from the first site to the second, and once with the propagation direction reversed. Both O-mode and X-mode rays are traced for each direction.

For the Chesapeake–Auburn analysis (`Simulation_Selector␣=␣3`), the script first computes the bearing and initializes the ionospheric model for the Chesapeake-to-Auburn direction. A full frequency sweep is performed for both O-mode (`OX_mode␣=␣1`) and X-mode (`OX_mode␣=␣-1`), extracting the closest valid ray at each frequency and computing the virtual reflection height from the geometric path length with Earth curvature correction. These results are labeled as the "True" direction. The process is then repeated with the roles of source and destination reversed (Auburn-to-Chesapeake), yielding results labeled as the "Reverse" direction.

For the Corpus Christi–Auburn analysis (`Simulation_Selector␣=␣4`), an identical procedure is followed. The maximum distance error tolerance is set to 100 km for all anisotropy simulations, as the relaxed constraint is necessary to capture sufficient data across the full frequency range for both propagation directions.

4.2 Results: Chesapeake ↔ Auburn

The anisotropy analysis for the Chesapeake–Auburn path produces two comparison plots. The first compares the calculated X-mode reflection height (derived from the geometric path) for the Chesapeake-to-Auburn direction against the Auburn-to-Chesapeake direction. The second plot provides the same comparison for the O-mode.

If the ionosphere were isotropic (or if the geomagnetic field had no effect), the forward and reverse traces would produce identical virtual height profiles. Any deviation between the two traces is therefore a direct indicator of the anisotropic influence of the geomagnetic field. The X-mode is expected to show greater sensitivity to direction reversal than the O-mode because the extraordinary wave's refractive index depends more strongly on the angle between the wave vector and the magnetic field. The magnitude and frequency-dependence of the observed differences provide insight into the strength and geometry of the geomagnetic field along the propagation path.

4.3 Results: Corpus Christi ↔ Auburn

The same analysis is performed for the Corpus Christi–Auburn path. Because this path has a different orientation relative to the geomagnetic field (running roughly east-west compared to the more northeast-southwest Chesapeake–Auburn path), the anisotropy signature is expected to differ.

Comparing the results from the two paths allows for a qualitative assessment of how path geometry relative to the geomagnetic field influences the degree of observed anisotropy. Paths that are more closely aligned with the magnetic field direction may exhibit less anisotropy than paths that are more perpendicular to it. This analysis demonstrates that the assumption of reciprocity, which is implicit in the 2D ray tracing model and in many simplified treatments of HF propagation, does not strictly hold in the real ionosphere.

5 Further Uses of PHaRLAP and Ray Tracing

The work presented in this report represents a subset of the analyses that can be performed using the PHaRLAP ray tracing toolbox. Several additional capabilities and extensions are worth noting.

5.1 Ionogram Inversion and Electron Density Profiling

One of the most important practical applications of oblique ionograms is the inversion of virtual height data to recover the true electron density profile of the ionosphere. The virtual heights computed in Sections 2 and 3 are not true heights but rather effective heights that include contributions from the group delay accumulated as the signal passes through the ionospheric plasma. Techniques such as the Abel inversion or polynomial-based methods can be applied to the virtual height–frequency relationship to extract the true height profile of electron density. PHaRLAP's ability to generate synthetic ionograms with known ionospheric conditions provides a valuable testbed for validating and refining such inversion algorithms.

5.2 Multi-Hop Propagation

The simulations in this report were restricted to single-hop propagation (`nhops␣=␣1`). PHaRLAP supports multi-hop ray tracing, which is essential for modeling long-distance HF communication paths that require multiple reflections between the ionosphere and the ground. Extending the analysis to multi-hop scenarios would enable the study of skip zones, signal focusing and defocusing effects, and the viability of very long distance communication links.

5.3 Absorption and Signal Strength Estimation

PHaRLAP provides collision frequency data that is used internally to model absorption of the radio wave as it passes through the ionospheric D-region and lower E-region. The absorption experienced by each ray can be extracted from the ray tracing output and used to estimate received signal strength. This information is critical for link budget calculations and for predicting the usability of a given frequency over a given path at a particular time of day and level of solar activity.

5.4 Temporal Variability Studies

The simulations presented here were all performed for a single time instant (July 1, 2004 at 10:00 UTC). By running the ray tracing procedure at multiple times throughout the day, a study of the diurnal variation of the ionogram and the MUF could be conducted. Such a study would reveal the strong dependence of ionospheric propagation on solar zenith angle and would demonstrate phenomena such as the post-sunset enhancement of the F-region and the disappearance of D-region absorption at night.

5.5 Real-Time Ionospheric Monitoring

The methodology developed in this project could be applied to real-time data from operational ionosondes and HF radar systems. By comparing observed oblique ionograms with ray-traced synthetic ionograms, discrepancies between the model and reality can be identified, potentially revealing the presence of ionospheric irregularities, traveling ionospheric disturbances, or space weather effects that are not captured by the background ionospheric model.

References

[1] M. Cervera, *Pharlap - provision of high-frequency raytracing laboratory for propagation studies*, Apr. 2024. [Online]. Available: `https://www.dst.defence.gov.au/our-technologies/pharlap-provision-high-frequency-raytracing-laboratory-propagation-studies`